

Feasibility Investigation and Modeling Analysis of CO₂ Sequestration in Arbuckle Formation Utilizing Salt Water Disposal Wells

Jamal Daneshfar¹, Richard G. Hughes², and Faruk Civan¹

1: The University of Oklahoma; 2: Louisiana State University

Abstract

Rate of CO₂ production in many states, primarily from coal-fired power plants, is such that it only takes a few years to fill up any depleted oil and gas reservoirs. In order to reduce the level of CO₂ in the atmosphere and to minimize the cost of sequestration, the injection of CO₂ into aquifers utilizing disposal wells has been targeted. In this paper, an analysis of one particular case, namely the Arbuckle formation in Oklahoma, is carried out to demonstrate its feasibility for CO₂ sequestration.

First, a general review for CO₂ sequestration into aquifers utilizing existing disposal wells is presented. The limiting criteria for CO₂ sequestration in terms of the geology of the aquifer, lithology of the host rock, cost of operation, impact on reservoir properties, depth of the completed interval to maintain super-critical conditions for CO₂, injection pressure and rate to minimize gravity segregation, mobility ratio to prevent viscous fingering, and chemical interaction of aqueous and solid phases are discussed. Then, the existence of residual oil in the aquifer and its effect on reaction chemistry concerning the potential CO₂ sequestration applications in the Arbuckle formation are investigated by means of simulation of the prevailing processes. The cut-off point from dissolution to precipitation for each constituent in terms of different CO₂ injection rates are obtained by utilizing the simulation models GEM-GHG and PHREEQC and incorporated into an analysis from a database of 150 disposal wells from which 25 wells are completed into Arbuckle Formation. The report critically evaluates the current state of knowledge, identifies areas needing research, and offers practical approaches for evaluation of potential CO₂ sequestration sites using commercial disposal wells.

Introduction

Carbon dioxide sequestration into subsurface formations, such as depleted petroleum reservoirs and ground-water aquifers, is being explored to avoid the release of CO₂ generated by the combustion of fossil fuels into the atmosphere. Presently, CO₂ injection into oil reservoirs based on conventional upstream oil and gas technology is being applied as an economically viable utilization and subsurface storage of CO₂¹. This method can provide additional recovery in the amount up to 40% of the residual oil left in reservoirs following primary recovery and subsequent water flooding. However, the CO₂ storage capability of this approach is very limited because a large fraction of the injected CO₂ eventually comes back along with the produced oil at production wells.

In an effort to alleviate this problem, in situ disposal of CO₂ into deep saline aquifers has gained much interest recently because high density CO₂ can dissolve in large quantities in formation water at elevated pressures. Adversely, however, injection of large volumes of CO₂ may increase the in situ pore pressure to such critical levels that the integrity and safety of the subsurface formations may be jeopardized. Further, the seals required for containing the CO₂ in aquifers are not as well understood as they are for oil and gas reservoirs.

One possible starting location for conducting commercial aquifer sequestration could be to convert existing commercial disposal wells to allow for CO₂ injection. Unfortunately, however, geological formations are not large enough to be the final storage for the CO₂ sequestration because of the limited capacity of all currently available depleted reservoirs and the time required for other reservoirs to be completely abandoned. Koide et al² pointed out that burning about 1 ft³ of petroleum product produces 2.2 ft³ of carbon dioxide, and hence oil reservoirs can store less than one half of the carbon dioxide that would be produced by burning the extracted product. Winter and Bergman³ show that CO₂ injection into all depleted reservoirs present in the US will take about 1.5 years to fill up considering the fact that half of the CO₂ is emitted east of the Mississippi River and most of potential disposal sites are west of the Mississippi. Performing a similar calculation for the state of Oklahoma suggests that the rate of CO₂ emissions from power plants (shown in Figure 1) would fill the estimated capacity of depleted reservoirs in about 3.5 years.

In view of the limited capacity of depleted petroleum reservoirs, saline aquifers in Oklahoma may be an option to sequester the CO₂ without interfering with the oil and gas reservoirs and is the focus of the present study. While a variety of potential operational difficulties are expected with such a conversion, this paper focuses primarily on aspects of the aquifer response. An analysis of a typical case is carried out to demonstrate the utilization of commercial disposal wells for CO₂ sequestration. The effect of residual oil in the aquifer on chemical interactions is investigated. The cut-off point from dissolution to precipitation for several constituents is determined by utilizing the GEM-GHG and PHREEQC geochemical-compositional numerical simulators. First, we present the aquifer response to CO₂ injection in the absence of a residual hydrocarbon phase. This case is similar to many cases presented in the literature^{4,5,6}. Then, we add an additional low saturation hydrocarbon phase into the mixture and compare the resulting precipitation and dissolution patterns.

Site Selection Criteria

Many factors in selecting sites for CO₂ sequestration into aquifers have been reviewed in the literature. These factors are reexamined here by incorporating actual field data from the Arbuckle formation in Oklahoma.

Geology

Oliver⁷ suggested that sites in divergent-sedimentary basins with low tectonic instability and high porosity and permeability were preferable to sites in convergent basins with crystalline rocks and few continuous seals. Higher permeability near well-bores allows better injection rates and less risk for fracturing the formation. However, lower permeability leads to higher residence time and less chance for the CO₂ to escape to upper layers and move toward the ground surface. Permeability has a linear relation with volume of CO₂ injected and porosity has a smaller effect compared to permeability. Hence, doubling the porosity from 6% to 12%, the volume of CO₂ injected raised only by about 7% in 30 years. Permeability values in the Arbuckle formation reported from many disposal wells are in the range of 30-60 md while porosity values range from 10-18%. The vertical permeability has been measured in one location as 25 md (lower than horizontal permeability) indicating the lower potential for gas moving upward during the process.

Neutzil and Pollack⁸ recommend selection of injection sites at a recharge area of a continental basin to increase the residential time as formation water flows from recharge areas with higher pressure (close to hydrostatic pressure) to discharge areas with lower pressure. Gunter et al⁹ examine the displacement mechanisms as CO₂ is injected into an aquifer as being molecular diffusion and dispersion, mixing with formation water and gravity segregation and viscous fingering. Gunter et al⁶ pointed out that dissolution is the predominant process at early stages of injection into siliciclastic aquifers and is the only process in carbonate aquifer injection leading to porosity and permeability increases as CO₂ is injected. In terms of geology, the Arbuckle formation is dominantly a carbonate lithology and will be more dolomitized moving toward the north-northeast part of the State where the majority of disposal wells are located.

Water Chemistry

Considering its physical properties and phase behavior, CO₂ will be in a supercritical state at in situ temperatures typically above 87⁰ F and pressures above 1200p. Hence, the CO₂ will have a gaseous behavior but a liquid density. Owing to prevailing geothermal and hydrostatic conditions, the CO₂ will reach supercritical conditions at depths greater than 2500 ft. This provides the conditions necessary to avoid the CO₂ separation into liquid and gas phase. Law and Bachu⁶ indicated that up to 25 % of CO₂ would dissolve into the formation water and then travel within the hydrodynamic system. The rest of the injected CO₂ will remain in an immiscible phase and has the tendency for gravity segregation and viscous fingering due to viscosity and gravity differences between the CO₂ and aqueous phases. Law and Bachu⁶ determined that the mobility difference, diminishing with depth, creates a large contact zone with the formation water and low permeability leads to propagation of about 3 miles after a period of 30 years injection.

The salinity of formation water is another important factor. Brine with total dissolved solids (TDS) greater than 100,000 mg/L absorbs less CO₂ compared with brackish water with TDS between 1,000-10,000 mg/L. Halloway and Savage¹⁰ reported the acid created by the CO₂ injection could be neutralized by carbonate minerals dissolved into the fluid leading to 1-4% increase in CO₂ storage capacity. This may cause formation damage due to removal of carbonate cement. However, siliciclastic aquifers can absorb more CO₂ through dissolution in water-rock reactions and lead to precipitation and trapping of carbonate minerals.

Formation Selected for Field Case

In this section, the various aspects of the Arbuckle formation considered for the present study are discussed.

Geology

The Arbuckle formation in Oklahoma is part of the Arbuckle group of late Cambrian and Ordovician age and was deposited as a carbonate platform that extended from west Texas to eastern North America. It is composed of a very thick and almost pure carbonate that is often dolomitized with the highest porosity and permeability rocks in the Mid-continent region. Johnson and Campbell¹¹ identified the Woodford Shale as having the best potential seal for the Arbuckle formation. The rock mineralogy of the formation is mainly dolomite, cherty dolomite and calcite with minor amounts of quartz sand. Ham¹² has reported that the carbonates in the Arbuckle group in southern Oklahoma are predominantly limestone, while those in northern part of the State are dolomitized.

With support from the Oklahoma Geological Survey, cores from the Arbuckle formation in the north-north-eastern part of the State were selected and one core, close to the location of many disposal wells was examined by the Fourier Transform Infrared Spectroscopy (FTIR) imaging technique at the University of Oklahoma. The results indicated almost 90% of the core is dolomite and the rest ranging from 1 to 4 percent is calcite, illite, quartz, and pyrite. The results from FTIR test are listed in Table 1.

Water Chemistry

Water samples from 250 brine wells in Oklahoma shows that the salinity ranges from 27,000 mg/L to 100,000 mg/L with carbonate rocks as the dominant rock type. This makes the Arbuckle an interesting target for the sequestration of the CO₂ emissions from Oklahoma power plants.

The large number of wells completed in the Arbuckle in Oklahoma provides access to the information necessary for the evaluation of the zone for CO₂ sequestration. The location of the majority of these wells is in the vicinity of the power plants, as shown in Figure 2, and may provide the opportunity to

sequester CO₂ emitted from the power plants with minimal transportation costs. The water samples from these wells taken over the years establish a database for different ion components and can be used to monitor the distribution of the different components before and after the actual injection.

The water is a calcium-magnesium-bicarbonate type, which undergoes reaction with injected CO₂ and changes the thermodynamic equilibrium that already exists. The database of water samples from brine wells in Oklahoma shows the average concentration of different ion species before CO₂ reaction (Figure 3). The major species are Ca⁺⁺, Mg⁺⁺, and Cl⁻ with average concentrations of 15,000 mg/l, 2,200 mg/l, and 125,000 mg/l, respectively.

Besides those brine wells completed in the Arbuckle formation, there are currently more than 25 wells completed in the Arbuckle formation in Oklahoma as disposal wells. The water production from different productive zones and/or water-flooding units in the State is injected into the Arbuckle utilizing these disposal wells. The completion depth ranges from 1,500-7,000 ft with an average porosity between 10-18% and permeability in the range of 10-60 md. The analysis of injected fluid and information about completion depth is shown in Table 2.

Simulation Models

Two different simulation models were utilized to examine the reaction of injected CO₂ with the aquifer water. The effects on concentration and saturation index for different species at different time periods have been reviewed under the two different systems.

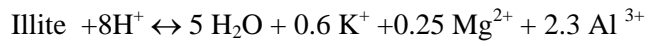
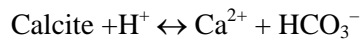
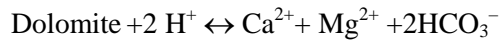
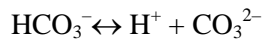
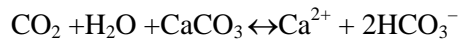
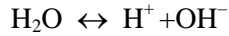
PHREEQC Geochemical Model

This software simulates a simple closed-tank model with the aquifer solution interacting with injected gas and without ion transport and flow through porous media. PHREEQC version 2 was utilized for this study¹³. This simulator calculates the concentration of elements, molalities, activities of aqueous species, pH, and saturation indices required to achieve an equilibrium system¹³. Reactions with different molar amounts of injected CO₂ were simulated until the system converges to equilibrium state. The objective was to examine the mean concentration of each component and use “average” Arbuckle aquifer water in our calculations. However, adjustments to this mean composition was needed in order to reach an equilibrium initialization. The range, mean and initial concentration values used in this study are shown in Table 3.

Various possible reactions between pore fluid and solid matrix and among ion species contained in the fluid solution may undergo by injecting CO₂ into the aquifer. Reactive fluid will dissolve solid minerals as it flows through porous media and will generate many different ions. Those ions may then

precipitate by reacting with other ions already present in the fluid when ion concentrations exceed the solubility of the precipitates. Then, this dissolution/precipitation process may alter the formation permeability and porosity^{15, 16}. Ion exchange processes can change the composition of ions in aqueous solution and pore surface, and therefore the structure of solid grains and porous matrix.

The chemical reactions between the injected CO₂ and solid minerals chosen for simulation were selected based on the Arbuckle FTIR tests and on the ion concentrations shown in Figure 3. The potentially essential reactions chosen were the following:



The simulation results shown in Figure 4 represent the molality for five selected major species and pH versus the pore volume of injected CO₂. The major species selected were Ca²⁺, Mg²⁺, H⁺, HCO₃⁻, and CO₃²⁻ and were based on the possible chemical reactions of injected CO₂ with aquifer water. The pore volume of injected CO₂ can be modified to a time scale based on the rate and volume of injection. These outputs were then reviewed to calculate changes in the saturation index from dissolution to precipitation and hence determine the minimum injection rate or volume before precipitation could happen for a particular species. This information will also help to indicate the percentage of injection gas as being free CO₂ or dissolved in the water leading to changes in injection schemes and improvement in the efficiency of CO₂ sequestration.

GEM-GHG Model

This is an open system equation-of-state compositional simulation model considering the effect of flow of CO₂ in the aquifer. The GEM-GHG simulator¹⁴ was utilized to examine the saturation of injected CO₂ and the changes of molality for different species during different time periods. In this option, the reaction of injected CO₂ with aquifer water and minerals from the host rock along with flow in a 2-dimensional system was considered. The aquifer was modeled using 1800 grid blocks (60×1×30 grid cells in the x, y, and z-directions) representing one portion of a 3-dimensional radial system as shown schematically in Figure 5. Grid cell sizes are 33×33×33 feet and this slice of the system represents 1/188 of the total model volume. Injection of CO₂ through one injection well (located at grid block 1, 1, 15) was modeled for ten years and then the well was shut in. To establish an equilibrium condition

prior to injection of CO₂, the well was initially kept shut in for a period of five years. The injection period and grid system were determined based on the storage capacity of 1-2 % of aquifer pore volume reported in the literature and the average life of power plants. All other input data are shown in Table 4 and are based on actual completion and aquifer data from an existing water disposal well in Oklahoma. The relative permeability curves used are shown in Figure 6 and are based on Stone's second model.

A total injection of 8.5 million tonnes of CO₂ through one injection well during the first ten years was simulated. Then, the well was shut in and the reactions of the minerals and aqueous solution were observed over a 500-year period.

Simulation Case Studies

In the following, the presence of residual oil in the aquifer and its effect on chemical reactions are considered. The reactions of injected CO₂ with aquifer water and their effects on concentration and saturation index for different species at different time periods are examined by means of these simulators. The cut-off point determination from dissolution to precipitation utilizing the GEM-GHG and PHREEQC numerical simulation models indicate similar trend for each constituent.

Fluid injected into disposal wells often contains some small percentage of hydrocarbon components. The accumulation of these hydrocarbon components over the years creates an oil zone around the well-bore and was the motivation to review the effect of residual oil on the reactions with the host rock. The GEM-GHG model was run with three different scenarios and the dissolution / precipitation of minerals and changes in gas and water mass density were examined. For each case, the gas saturation, mineral dissolution, water mass density and bottom hole pressure were plotted and results were compared to examine the effect of higher hydrocarbon presence around the well-bore.

Case One

The system was initialized with 99.5% water saturation, 0.5% gas saturation, and no residual oil. The water mass density, gas saturation, and mineral dissolution/precipitation were plotted as a base case, which then can be compared with the following cases. The minerals to be tracked were selected to be calcite, dolomite, and illite based on the FTIR results from the Arbuckle core sample.

The gas saturation for different layers at different times were examined and, as expected, most of the gas is located toward the upper portion of the model during the injection period and reaches to about 150 meters away from the injection site in almost 500 years. Gas saturation variations for the upper layer (layer 1), the middle layer, in which injection takes place, and the bottom layers were selected to demonstrate the effects of initial oil saturation. The upper layer gas saturation will be shown to be critical in terms of duration of gas presence after injection is over and the possibility of CO₂ escaping to

surrounding zones. After 100 years, the gas saturation fraction is 0.3 and 0.004 in the top and bottom layers, respectively.

The bottom-hole pressure reaches the imposed pressure constraint as injection continues for 10 years with no significant decline in pressure seen immediately after injection stopped. The bottom hole pressure gradually declines for all cases as shown in Figure 7 representing CO₂ migrating away from the gas plume or dissolving in the water. In this case, the cumulative number of moles of CO₂ remaining in the gas and aqueous phases will be 2.1 and 6.3 billion moles, respectively. It is observed that the CO₂ molality in the water phase is almost three times (75%) more than in the gas phase (25%) and that it takes almost 200 years for all of the CO₂ in the gas phase to dissolve. Figure 8 shows the trend of CO₂ moles in each phase for different cases.

Water mass density plots for the upper and lower layers show the effect of the dissolution of CO₂ into the aqueous phase (Figure 9). In the top layer, the water mass density increases by about 54 kg/m³ during the 10-year injection period and starts to decline once injection stops. The water mass density in the bottom layer is on an increasing trend at the end of the modeling period.

The dissolution / precipitation for each mineral at different layers and different time periods shows more dissolution of each mineral in the top layer (more gas presence) and less activity moving down toward lower layers (Figure 10). The negative saturation index indicates the dissolution of calcite drops from -40 in the top layer to -1.6 in the bottom layer during the 500-year model period. This implies even after 500 years calcite dissolution continues and needs more time to change to precipitation. For dolomite, the saturation index changes from -6 in the top layer to -0.18 in the bottom layer. However, illite did not show any dissolution during the process. The total moles of calcite and dolomite dissolved in the entire system was 92 and 18 million moles and the amount of illite precipitated was 0.29 million moles during the 500 year simulation.

Case Two

In this case, the system was initialized with initial 1% oil saturation with the oil modeled as a C7-C10, default hydrocarbon component as described in the GEM-GHG manual¹⁴. All other factors in terms of volume of gas injected, duration of injection and reservoir size remained the same. A plot of gas saturation for different layers shows high activity around the first 100 meters away from the well-bore (closer to the well-bore, compared to Case One). It did not distribute areally as occurred in Case One due to the solubility of CO₂ in the oil. The output also shows that the gas saturation reaches a lower value in a shorter period of time in the middle and bottom layers.

Due to the presence of the oil, the cumulative amount of CO₂ remaining in the oil+gas (27%) and in the aqueous phases (73%) was 1.97 and 5.25 billion moles, respectively. The CO₂ in the oil+gas phase takes almost 350 years to diminish which is longer compared to Case One. The mineral dissolution / precipitation activities represent less mineral dissolution during the 500 years and follow the same trend as gas saturation closer to the well-bore. The dissolution is farther away from the upper grid layers and the saturation index shows lower values as the process continues. The total moles of calcite and dolomite dissolved were 76 and 17 million moles and 4 million moles of illite precipitated for the 500-year simulation.

For calcite, the saturation index drops from -12 in the top layer to - 1.6 in the bottom layer. This is lower than in Case One. The lower dissolution values are more visible in the upper layer and the differences between Cases One and Two are almost imperceptible in the bottom layer. The presence of the oil in the top layer and the solubility of CO₂ in the oil cause less dissolution of mineral rock in the upper layers (less free CO₂ is available to react with minerals) and will be more in equilibrium towards the bottom layers.

For dolomite, the saturation index ranges from - 1.4 to - 0.2 from the top layer to the bottom layer during the process, which is again lower than in Case One and also starts to show precipitation about 190 years after the project was initiated. The total number of moles of dolomite precipitated in 300 years was 4 million moles; however, the total moles dissolved before precipitation was 13 million moles in a shorter time period. This indicates the rate of dissolution is faster than the rate of precipitation and requires more time to precipitate what is already dissolved.

For illite, the activity is again closer to the well-bore and almost twelve times more moles of illite are precipitated than in Case One. The saturation index changed from +50 in the top layer to +0.04 in the bottom layer in 500 years. This is higher than in Case One. The delay in mineral dissolution (calcite) and more mineral precipitation (dolomite and illite) has been seen in the system with a small initial oil saturation compared to the system with no initial saturation (Case One) owing to CO₂ solubility in the oil and the presence of less free CO₂ to participate in rock-fluid reactions. This helps the upper layers to remain in precipitation phase (no secondary CO₂ migration due to gravity differences) after injection stops.

Case Three

In this case, the initial water saturation was set to 95% the initial oil saturation was 4.5% and the initial gas saturation remained 0. 5%. This system shows overall activities covering a smaller area compared to the first and second cases. The gas saturation plots for different layers indicate that the gas distribution is closer to the well-bore (around 50m). The gas saturation is limited to the upper layers

and will be zero in the bottom layers throughout the process. Due to the increase in oil saturation, the number of moles of CO₂ in oil+gas phase is more than both Case One and Case Two and peaks at 3.1 billion moles. As Figure 8 shows, even after 500 years there are still about 20 million moles of CO₂ retained in the oil+gas phase.

The overall mineral dissolution / precipitation plots indicate lower saturation indices as water saturation dropped from 99.5% to 95%. The total moles of calcite and dolomite dissolved were 68 and 39 million moles and the illite precipitation was 1.2 million moles. For calcite, the saturation index drops from – 2.5 in the top layer to –1.2 in the bottom layer. These values are much lower than the values seen in Case One and Case Two. The low saturation index in the top layer can be related to a larger hydrocarbon presence and the affinity of CO₂ to dissolve in the oil. As a result, less CO₂ will be available and less rock will be dissolved. The same trend was seen in Case Two.

Overall, the saturation index dropped from –0.1 in the top layer to –0.4 in the bottom layer in 500 years with no indication of dolomite precipitation as was seen in Case Two. For illite, the saturation index shows that precipitation occurs in all layers but at a lower rate. The index is lower in the upper layers (similar to calcite and dolomite) and then approaches a higher value than seen in Case Two towards the bottom layers.

The overall trend of dissolution / precipitation for each mineral and each case is shown in Figure 10. The plot shows that calcite dissolution is highest in Case One (no hydrocarbon present) and decreases as hydrocarbon presence increases. Dolomite precipitation occurred only in Case Two and illite precipitation was more significant in Case Two.

The effect of residual oil then is that it delays the rock-fluid reaction process and keeps the water mass density higher throughout the shut in period. CO₂ stays closer to the well-bore and does not propagate out into the formation nearly as far as when there is no oil present.

Final Remarks

The purpose of this study was to investigate the feasibility of CO₂ injection in the Arbuckle formation in Oklahoma utilizing commercial disposal wells. The emission from power plants is on an increasing trend and the limited capacity of depleted oil and gas reservoirs make them too small to be the final storage site for CO₂ sequestration. The location of power plants in the vicinity of disposal wells completed in the Arbuckle group may provide a practical application in terms of lower operational costs and availability of sources and sinks for CO₂ sequestration. The nature of the host rock and existence of the Woodford shale on the top of the aquifer could make these reasonably safe places for CO₂ sequestration for a long period.

Simulation results of CO₂ injection using parameters similar to those found in disposal wells completed in the Arbuckle formation indicate the reaction front will be in the vicinity of the well-bore and the trend of mineral dissolution / precipitation will be more uniform towards the bottom of the well. The presence of the residual oil delays mineral dissolution / precipitation and minimizes the area for gas saturation distribution to the vicinity of the well-bore. Due to CO₂ solubility in oil, the saturation index representing mineral dissolution or precipitation has lower values for all minerals studied in the upper layers and will be more uniform towards the bottom layers. The overall grid volume calculations show less mineral dissolution / precipitation as residual oil saturation increases. Dolomite precipitates part way through the shut in period in only one of the cases that were simulated (Case Two). Illite precipitation increased significantly as oil was introduced into the system. However the changes seen could not be correlated based on the limited number of runs performed.

There may be some critical oil saturation that adversely effects the mineral precipitation. Calcite dissolution fell as oil saturation increased, but never precipitated. The molality (mol/kg H₂O) of CO₂ in oil+gas and water phases at different time periods indicate the CO₂ will be retained in the aqueous phase even after 500 years. It diminishes in the oil+gas phase as early as 200 years without the presence of initial oil saturation and remains in the oil+gas phase as late as 500 years as oil saturation increased. The results also indicate that there is a drop in the CO₂ molality in the aqueous phase as CO₂ molality in the oil+gas phase increases. Further studies are necessary to evaluate the effect these dissolution / precipitation observations have on permeability and porosity.

ACKNOWLEDGMENT

Original Petroleum Society manuscript No. 2004-179 presented at the 55th Annual Technical Meeting, Calgary, AB, 8-10 June 2004. The attached material is being used with permission as published by the Petroleum Society. The author thanks the Petroleum Society for the use of this material and reminds recipients that copyright remains with the Petroleum Society and that no other copies may be made without the expressed written consent of the Petroleum Society.

The author also thanks the Sixth Annual Conference on Carbon Capture and Sequestration for the permission to attach the material presented in Pittsburg during May 7-10, 2007.

REFERENCES

1. Reichel, D., "Carbon Sequestration Research and Development", U.S. Department of Energy Report DOE/SC/FE-1, Washington, DC, 1999
2. Koide, H., Tazaki, Y., Noguchi, Y., Masaki, I., Kazuitsu, I, Shindo, Y., "Underground Storage of Carbon Dioxide in Depleted Natural Gas Reservoirs and in Useless Aquifers", Engineering Geology, 34(1993) 175-179

3. Winter, E.M, Bergman, P.D, "Availability of Depleted Oil and Gas Reservoirs for disposal of carbon dioxide in the United States", U.S. Department of Energy, Pittsburgh Energy Technology Center
4. Nghiem, L., et al.: "Simulation of CO₂ EOR and Sequestration Processes with a Geochemical EOS Compositional Simulator", Paper 2004-051 in the Proceedings of the Canadian International Petroleum Conference, Calgary, Alberta, Canada, June 8-10, 2004.
5. Holtz, M.H., et al.: "Reservoir Simulation of CO₂ Storage in Deep Saline Aquifers", proceedings of the Third Annual NETL Conference on Carbon Sequestration, Alexandria, VA, May 3-6, 2004.
6. Law, D.H.S., Bachu, S., "Hydrological and Numerical Analysis of CO₂ Disposal in Deep Aquifers in the Alberta Sedimentary Basin", Alberta Research Center
7. Oliver, J., "Fluids Expelled Tectonically from Organic Belts: Their Role in Hydrocarbon Migration and other Geologic Phenomena", *Geology* 1986; 14:99-102
8. Neuzil, C.E., Pollock, D.W., "Erosional Unloading and other Geologic Phenomena", *Geology* 1986; 14:99-102
9. Gunter, W., Perkins, E., McCain, T., "Aquifer Disposal of CO₂ Rich Gases: Reaction Design for Added Capacity", *Energy Conversion and Management*, vol. 34, no. 9-11, pp. 941-948, 1993
10. Holloway, S., Savage, D. "The Potential of Aquifer Disposal of Carbon Dioxide in the UK", *Energy Conversion and Management*, vol. 34, no. 9-11, pp. 925-932, 1993
11. Johnson, K., Campbell, J., "Petroleum-reservoir geology in the southern Mid-continent", Symposium Proceeding, March 6-7, 1991, Norman, Oklahoma
12. Ham, W.E., "Origin of Dolomite In the Arbuckle Group, Arbuckle Mountains, Oklahoma, in Moore, C.A.(ed), Proceedings of the Fourth Symposium on Subsurface Geology, University of Oklahoma
13. Parkhurst, D.L.: "User's guide to PHREEQC; a computer program for speciation, reaction-path, advective-transport, and inverse geochemical calculations", Water-Resources Investigations - U. S. Geological Survey, Report: WRI 95-4227, 1995.
14. Computer Modelling Group Ltd.: "Users Guide – GEM-GHG version 2005", Calgary, Canada.
15. Civan, F., "Scale Effect on Porosity and Permeability- Kinetics, Model, and Correlation," *AIChE J.*, Vol. 47, No. 2, pp. 271-287, February 2001.
16. Civan, F., *Reservoir Formation Damage-Fundamentals, Modeling, Assessment, and Mitigation*, 2nd Ed., Gulf Professional Pub., Elsevier, 1114 p, 2007.
17. Oklahoma Corporation Commission, "UIC Disposal well Data Base", April 2005
18. U.S. Department of Energy, Office of Fossil Energy, "U.S. Brine wells Data Base", 2003
19. U.S. Department of Energy, Energy Information Administration, "Power Plant Data Base", 2005

Table 1 FTIR Results for Arbuckle Core sample

Depth	Quartz	Calcite	Dolomite	Illite	Smectite	Kaolinite	Chlorite	Pyrite	Ortho	Oligio	Mixed	Albite	Anhydrite	Siderite
2364	0	2	94	0	0	0	0	3	0	0	1	0	0	0
2365	4	3	84	0	3	0	0	4	2	0	0	0	0	0
2367	1	1	94	2	0	1	0	0	1	0	0	0	0	0
2369	3	2	88	3	0	0	0	2	2	0	0	0	0	0
Average	2	2	90	1.25	0.75	0.25	0	2.25	1.25	0	0.25	0	0	0

Table 2 Completion data for Commercial Disposal Wells

API	Inj. Rate(bbl/d)	Pressure	Treatable Water Base	TDS	Cl-	Perf.Top	Perf.Bottom	φ	K
20422	10000	1000	450	188890	111503	7153	8750	15	10
28159	6000	1000	375	145500	87300	3830	4200	0	0
75027	3000	700	250	0	0	2706	3060	0	0
23783	4500	1800	336	46200	27700	3633	4900	18	37
1441	6000	600	670	0	0	3834	4144	0	0
22309	6000	1000	350	0	0	4700	4800	0	0
27971	3000	500	450	0	46036	1335	1355	16	0
37654	10000	0	850	226400	143573	6518	6818	0	0
22510	3000	800	280	0	0	3071	3856	0	0
20838	3000	800	550	0	0	2416	2900	0	0
22662	12000	250	160	0	0	4055	5047	0	0
21026	5000	300	300	0	0	5012	5869	0	0
21057	10000	0	323	0	0	5388	6499	0	0
21934	10000	500	350	0	0	5000	6300	0	0
22233	10000	1000	0	0	0	3950	0	0	0
21066	4000	600	350	0	0	1872	1882	0	0
22684	7000	700	350	0	0	1850	2000	18	59
23725	60000	750	680	156000	566000	5449	7334	7	
23412	3000	350	50			1490	1502	10	58
21599	5500	2200	485	171000	105000	7570	9078		
35633	0	0	775	0	0	7106	8835	0	0
22860	1000	1000	645	0	0	4355	5935	0	0
21631	5000	300	1050	0	0	5500	6500	0	0
22393	2000	1000	0			3872	3950		

Table 3 Ion Concentration from Brine Wells in Arbuckle Formation

Component	Concentration, mg/lit (Min)	Concentration, mg/lit (Max)	Concentration, mg/lit (Mean)	Input value, mol/kg-H2O
Na ⁺	2958	56000	52494	NA
Mg ⁺⁺	122	6225	2360	5.12E-05
Ca ⁺⁺	2520	23400	12507	5.61E-04
Cl ⁻	1048	175000	110467	NA
HCO ₃ ⁻	100	4400	227	4.04E-04
SO ₄ ⁻	100	4017	436	NA
pH	5.3	8.7	6.7	NA

Table 4 Reservoir data for Simulation Model (open System)

Reservoir Properties for CO ₂ Injection into Arbuckle Formation	
Grid	60*1*30
Grid Block Sizes	Dx = 33 ft, Dy = 33 ft, Dz = 33 ft
Horizontal Permeability	50 md
Vertical Permeability	25 md
Porosity	0.15
Depth of Reservoir Top	4000 ft
Reservoir Temperature	125 °F
Reservoir Pressure	1750 Psig @4000 ft

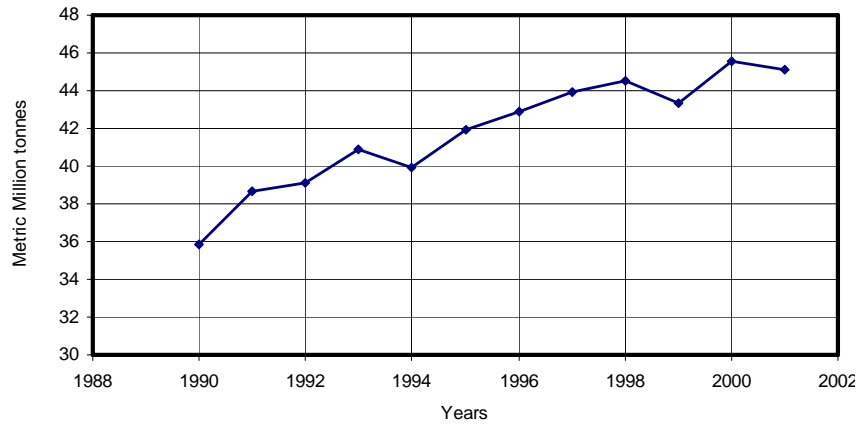


Figure 1 CO₂ emission trend from power plants in Oklahoma

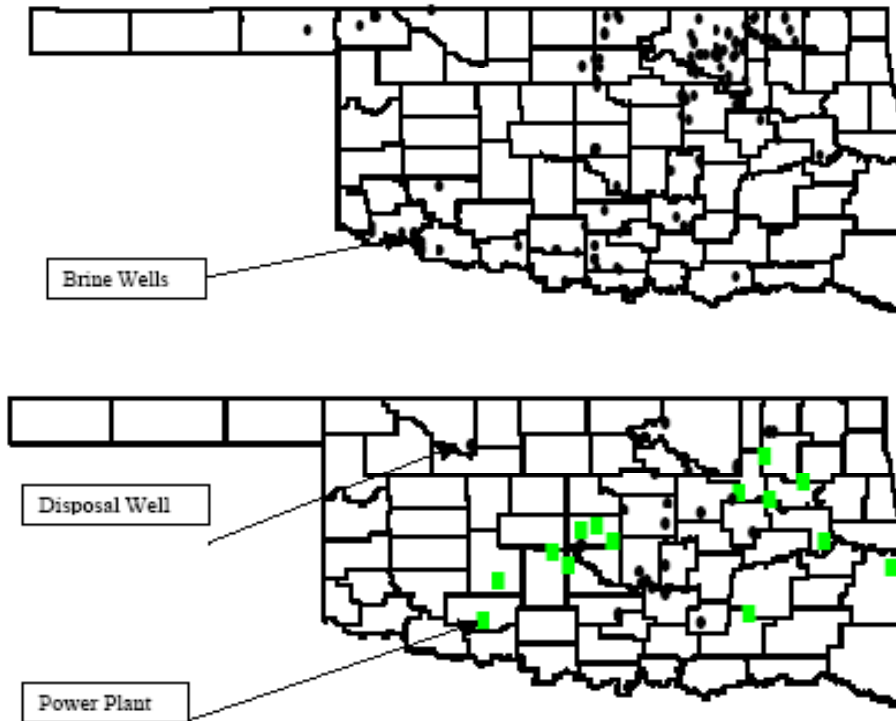


Figure 2 Locations of Brine¹⁸/Disposal Wells¹⁷ and Power Plants¹⁹ in Oklahoma (Created by ArcView GIS version 8.2)

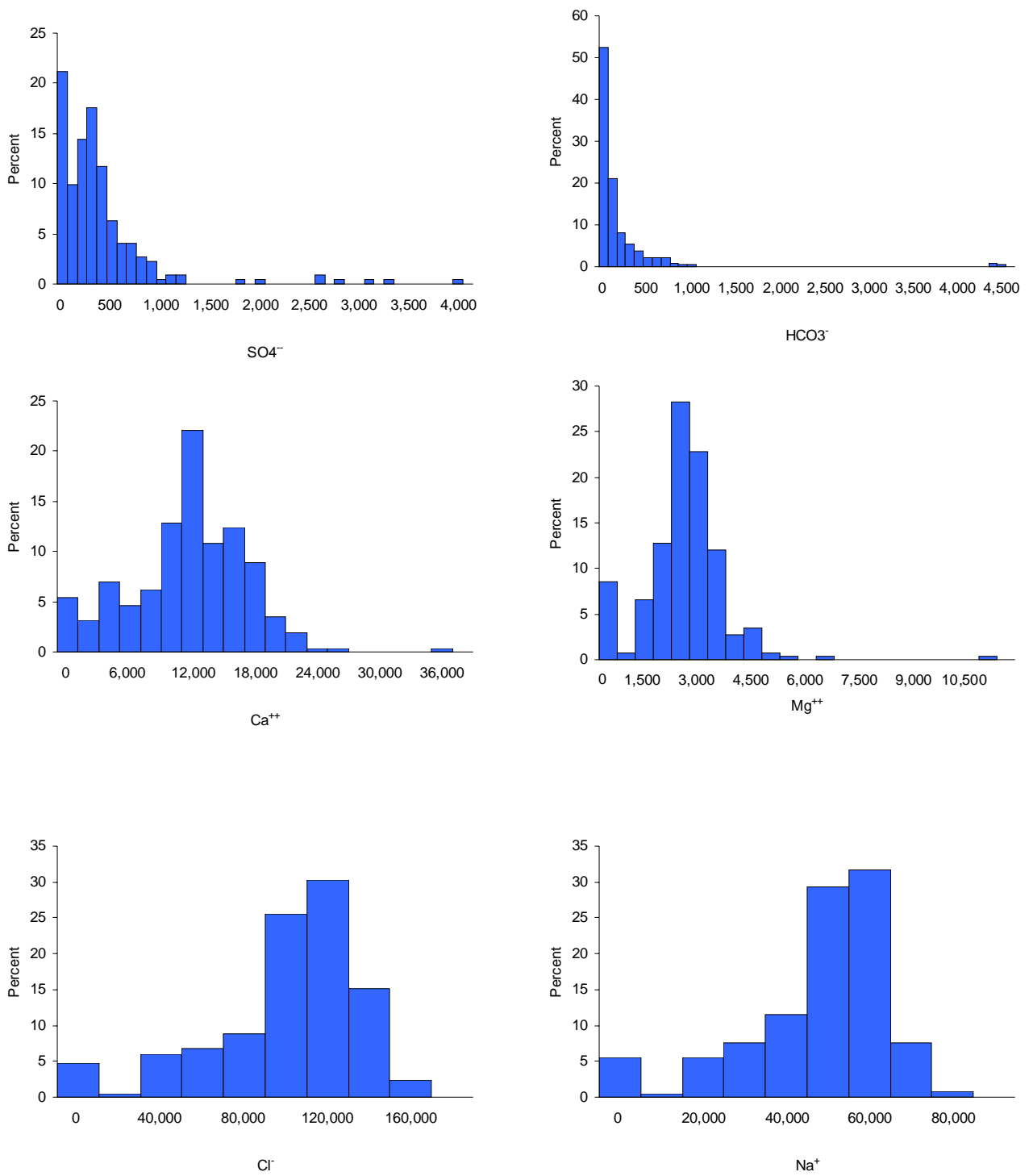


Figure 3 Ion Concentration Distributions before CO₂ Injection

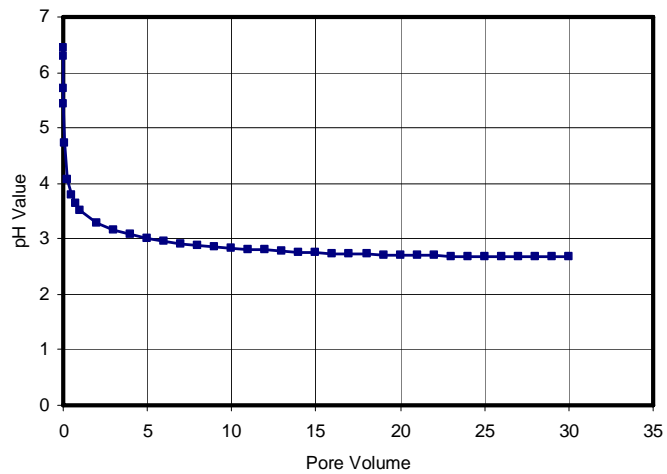
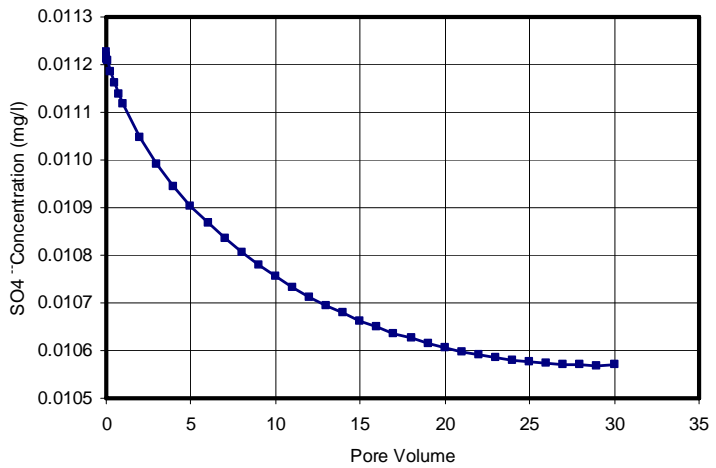
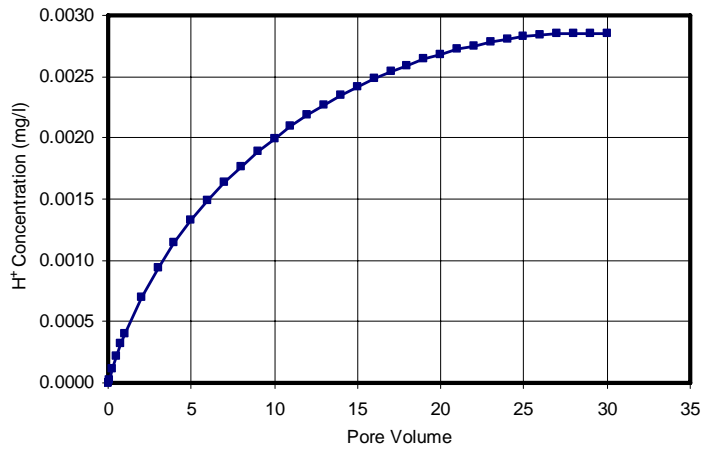
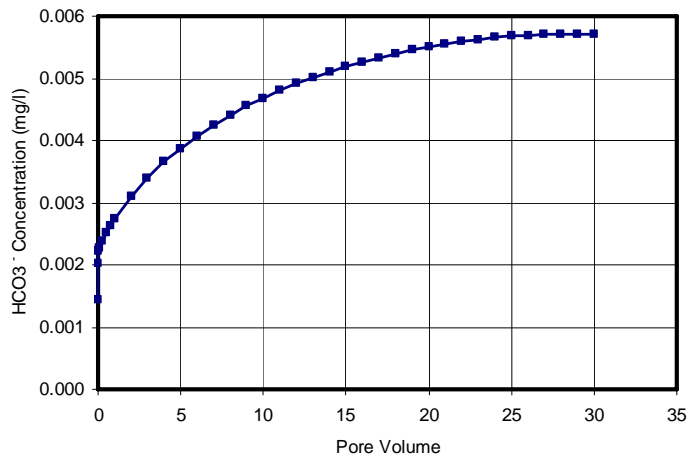
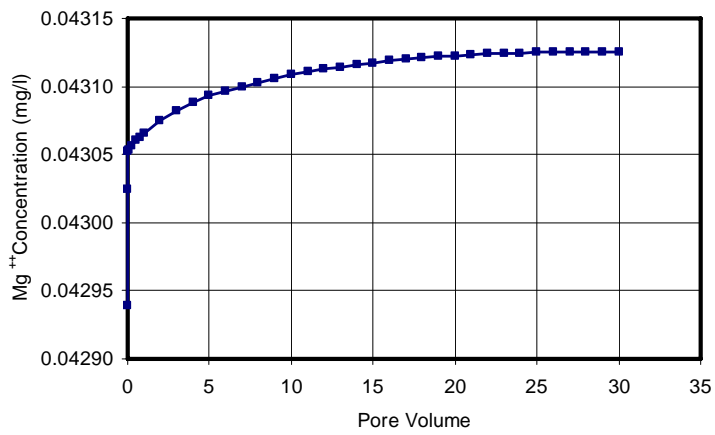
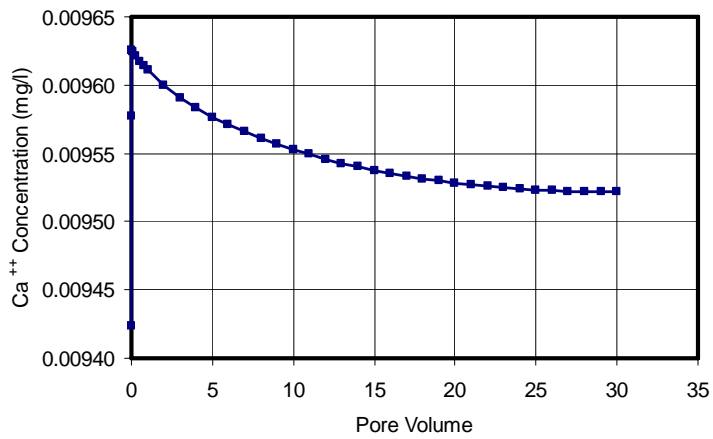


Figure 4 Average Ion Concentrations after CO₂ Reaction (Closed System)

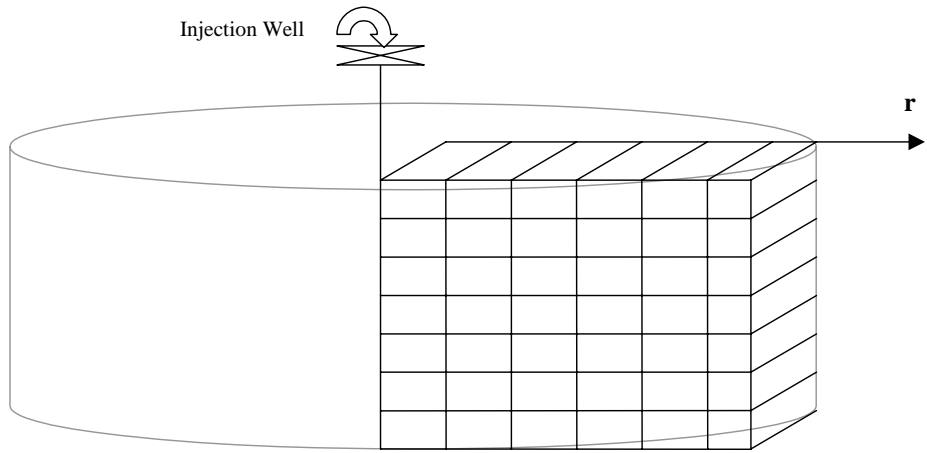


Figure 5 Grid Block System ($60 \times 1 \times 30$) in aquifer and simulation cases

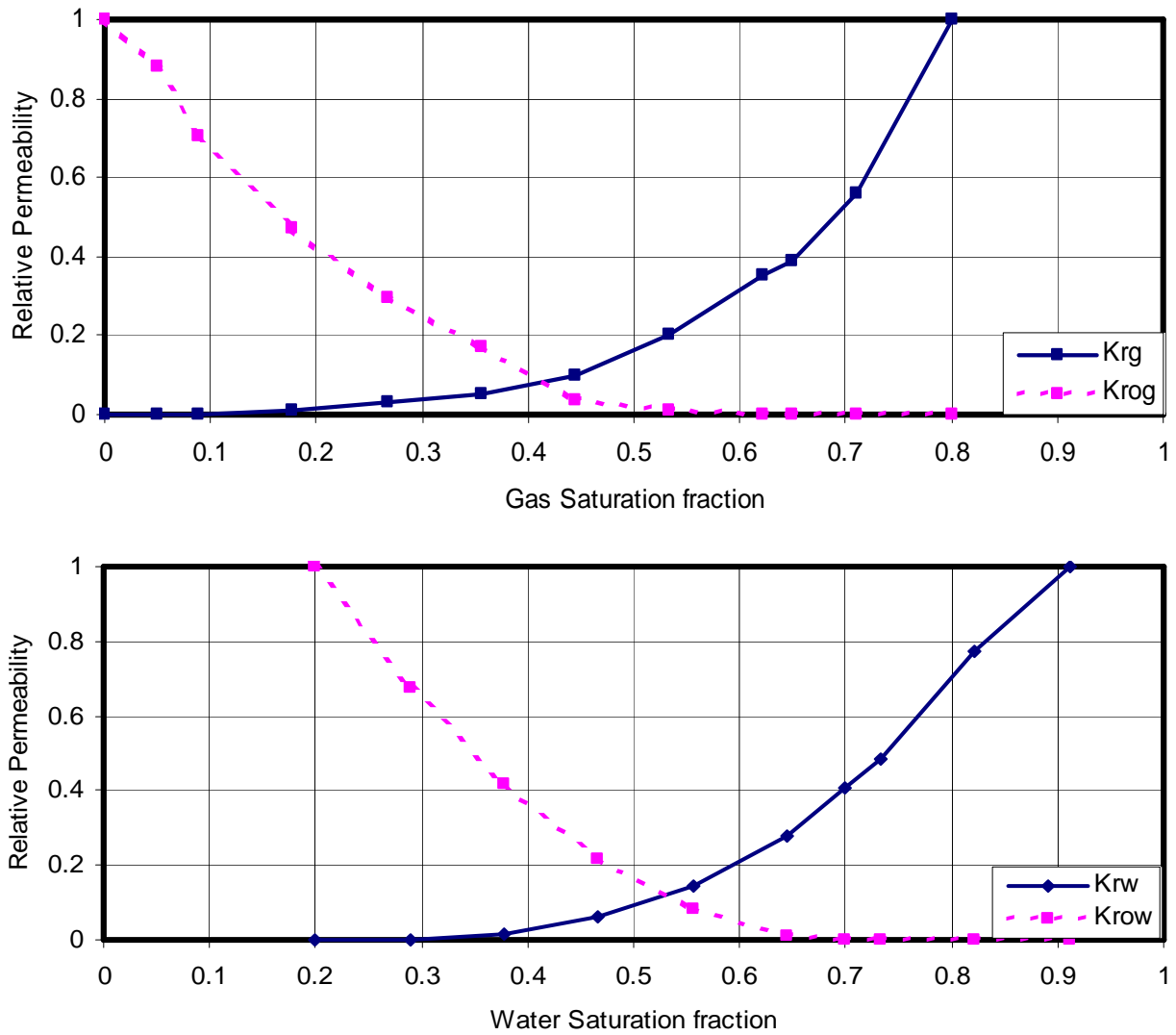


Figure 6 Relative Permeability (Based on Stone's Second Model¹⁴)

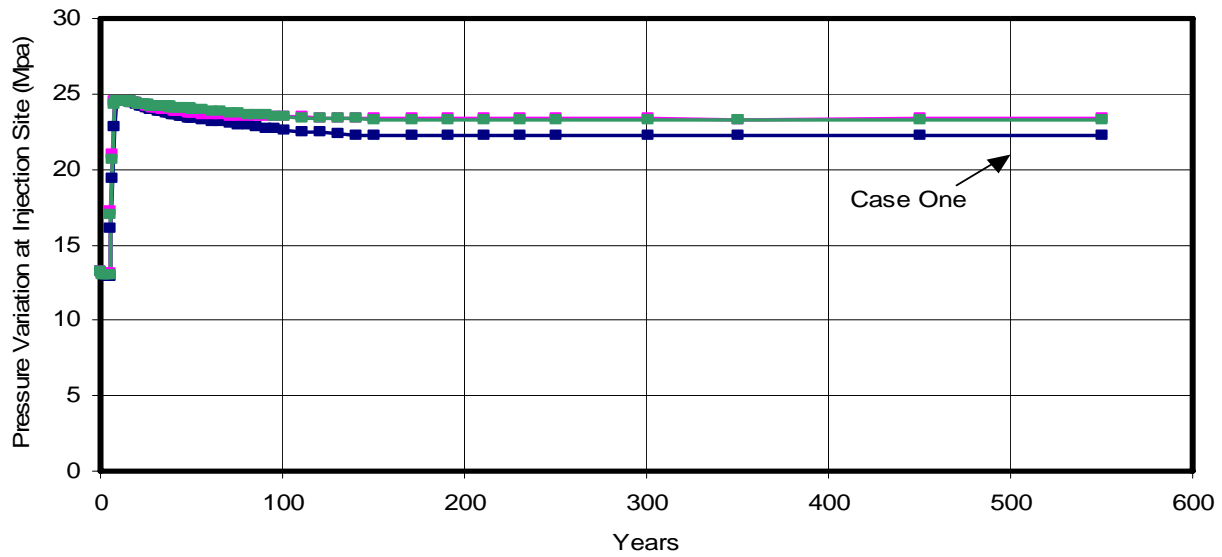


Figure 7 Pressure variations at Injection site –All cases

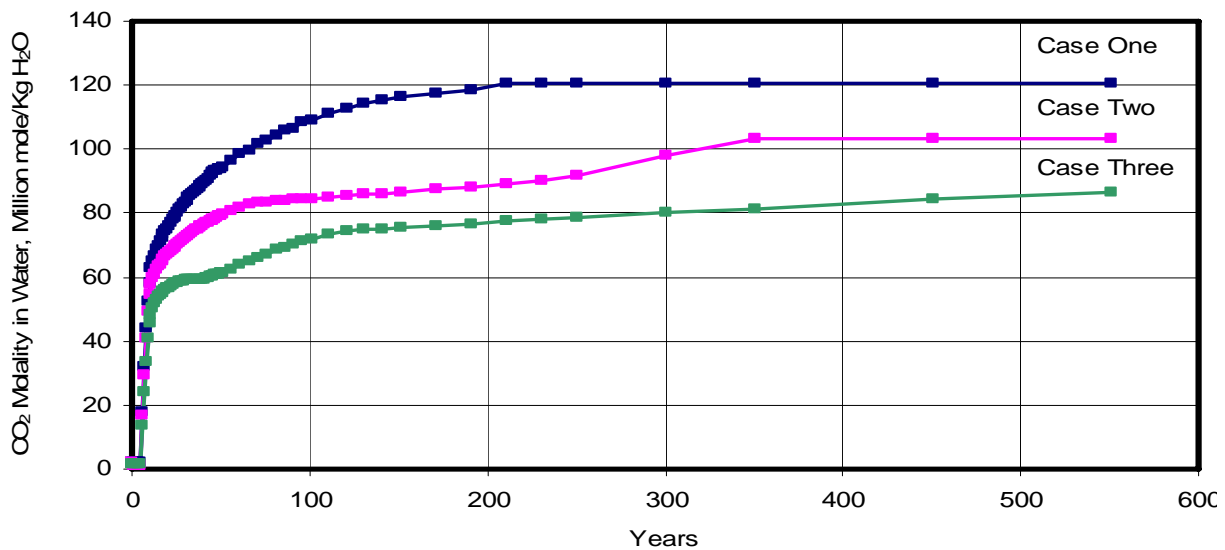
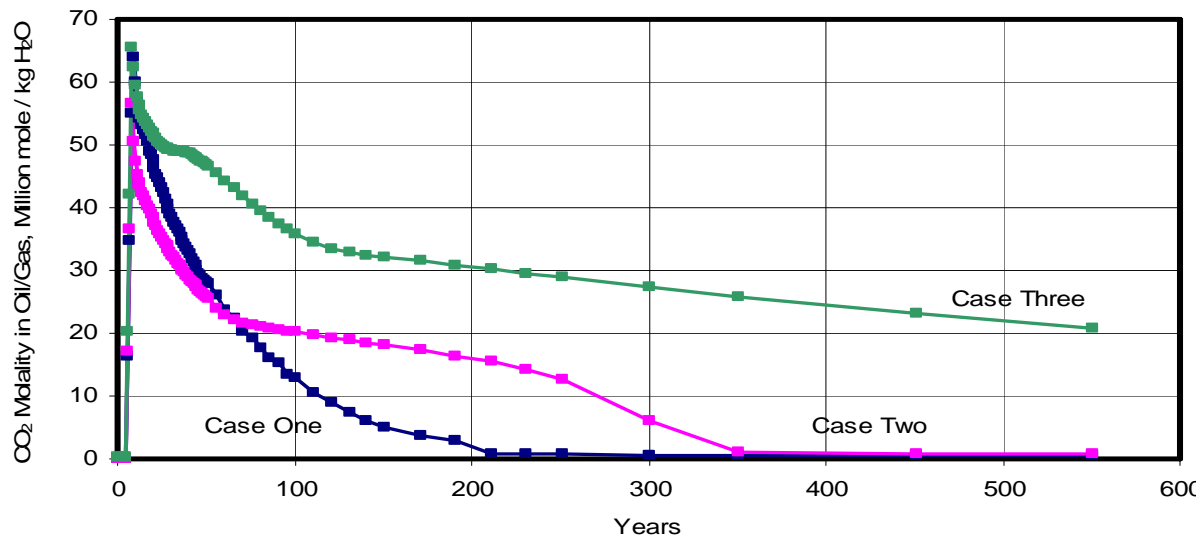


Figure 8 CO₂ Molality for Different Cases

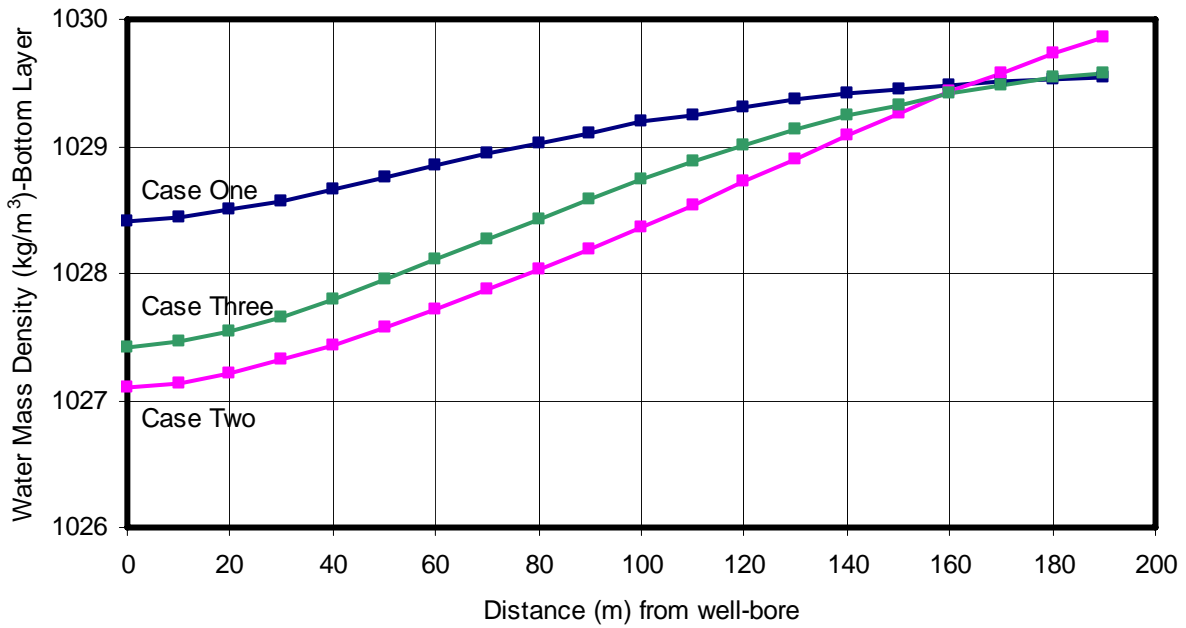
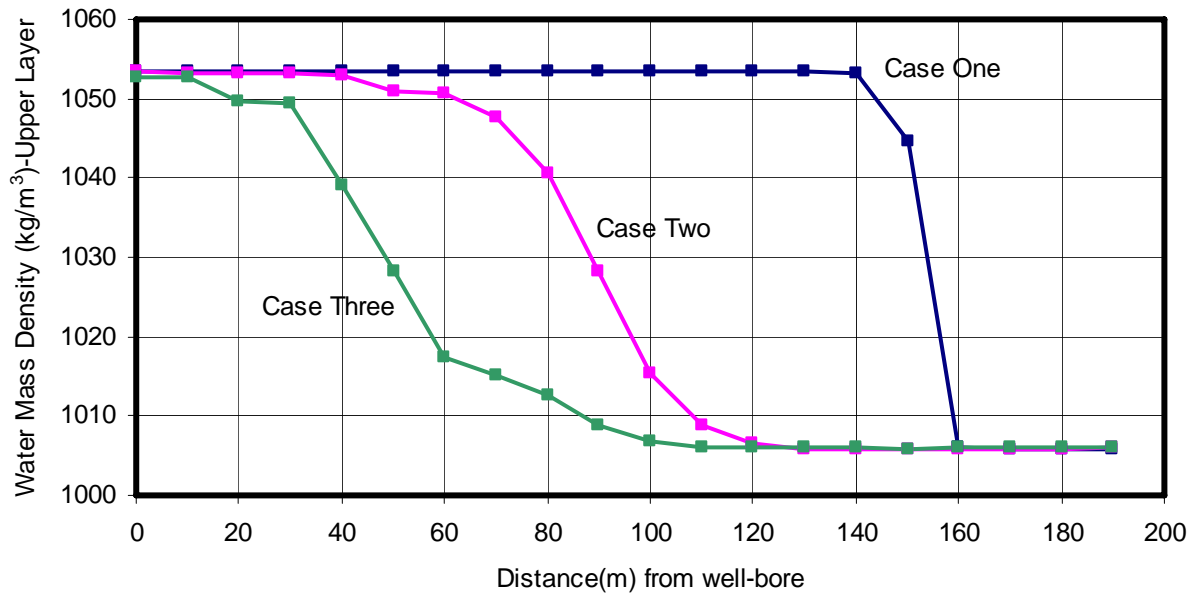


Figure 9 The Water Mass density in the Upper and Lower Layers

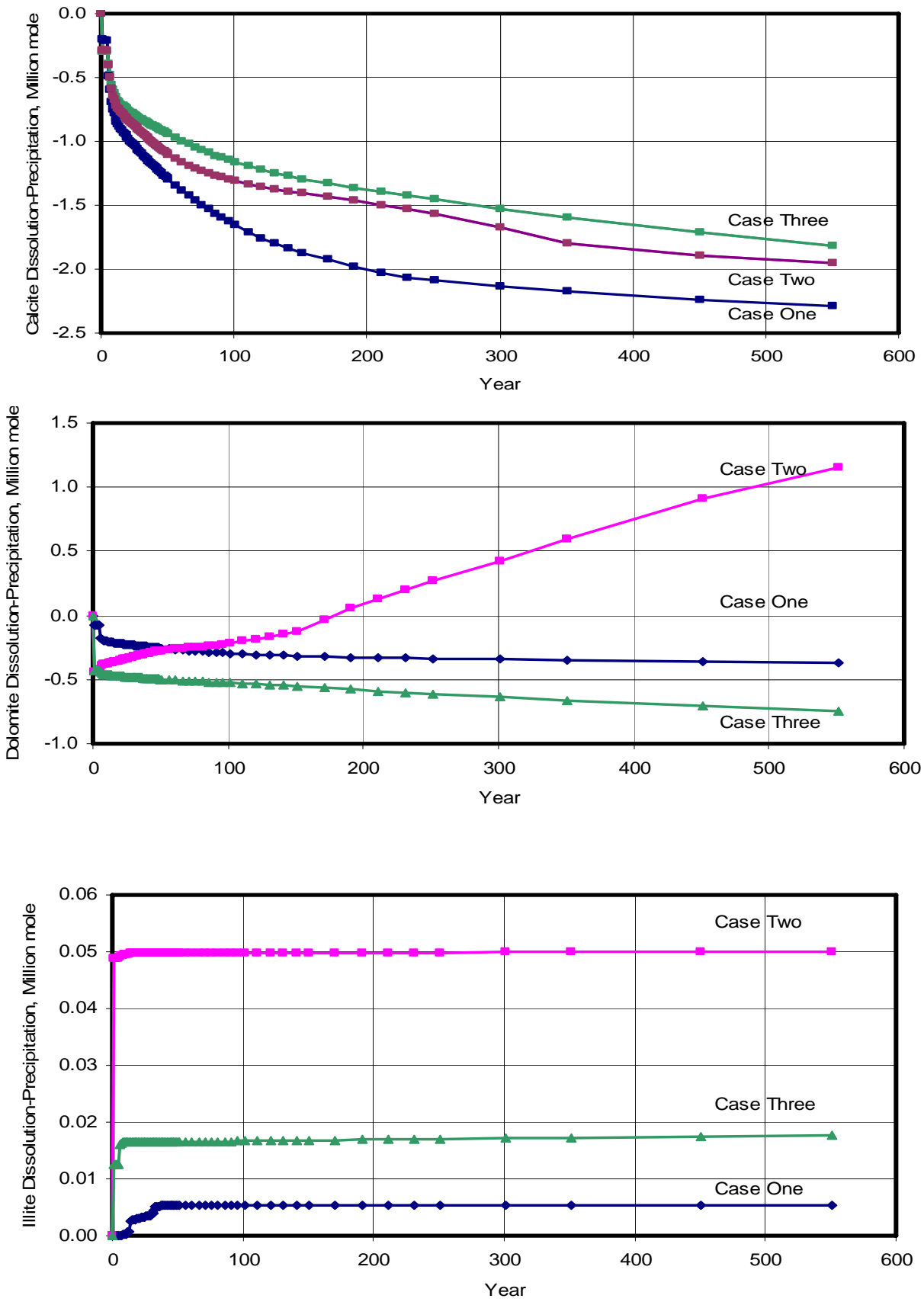


Figure 10 Mineral Variation for Different Cases